Taylor & Francis
Taylor & Francis Group

Canadian Water Resources Journal / Revue canadienne des ressources hydriques

ISSN: 0701-1784 (Print) 1918-1817 (Online) Journal homepage: http://www.tandfonline.com/loi/tcwr20

Modelling Climate Change Impacts on Spring Runoff for the Rocky Mountains of Montana and Alberta I: Model Development, Calibration and Historical Analysis

Robert P. Larson , James M. Byrne , Daniel L. Johnson , Matthew G. Letts & Stefan W. Kienzie

To cite this article: Robert P. Larson , James M. Byrne , Daniel L. Johnson , Matthew G. Letts & Stefan W. Kienzie (2011) Modelling Climate Change Impacts on Spring Runoff for the Rocky Mountains of Montana and Alberta I: Model Development, Calibration and Historical Analysis , Canadian Water Resources Journal / Revue canadienne des ressources hydriques, 36:1, 17-34, DOI: 10.4296/cwrj3601017

To link to this article: http://dx.doi.org/10.4296/cwrj3601017

Modelling Climate Change Impacts on Spring Runoff for the Rocky Mountains of Montana and Alberta I: Model Development, Calibration and Historical Analysis

Robert P. Larson, James M. Byrne, Daniel L. Johnson, Matthew G. Letts, and Stefan W. Kienzle

Abstract: Water supply from mountain snowmelt is a key resource on the Great Plains. Hydrologists recognize that water yields could be significantly reduced in a warmer climate, with negative impacts upon regional water supplies. Weather data availability is usually sparse in alpine watersheds. Consequently, distributed alpine snow hydrology models are generally limited to small instrumented watersheds. Such models are unable to simulate the timing and magnitude of spring streamflow at a sufficient spatial scale for watershed management. In this study, the Simulated Grid microclimate model (SIMGRID) was refined and applied to the simulation of snow water equivalent (SWE) and spring streamflow volume in the headwaters of the St. Mary basin of northern Montana. Relationships between winter precipitation and elevation were derived from snow survey data. The SWE mass balance algorithm was enhanced to include the effect of rain-on-snow conditions, and to differentiate between snowmelt and rainfall runoff. Multiple regression analysis was used to relate predicted SWE and rainfall runoff to observed stream discharge (Q_s) at Babb, MT, for the 1961-1990 period. The refined SIMGRID model was then applied to the 1991-2004 period, and accurately simulated spring discharge (linear regression, $r^2 = 0.67$). The refined SIMGRID model is capable of simulating spring runoff in poorly-instrumented complex terrain, at a scale of relevance to water resource managers. This paper presents the results of Part I of a two-part study, which assesses the impacts of climate change on spring runoff for the study watershed.

Résumé : L'approvisionnement en eau provenant de la fonte des neiges en région montagneuse est une ressource importante dans les Grandes Plaines de l'Amérique du Nord. Les hydrologistes reconnaissent que les débits des cours d'eau pourraient être sensiblement réduits dans un climat plus chaud, avec un impact négatif sur l'approvisionnement en eau à l'échelle régionale. En général, il existe peu de données météorologiques disponibles dans les bassins hydrographiques alpins. Par conséquent, les modèles hydrologiques de distribution nivale en milieu alpin se limitent généralement à de petits bassins versants instrumentés. Ces modèles ne permettent pas de simuler les variations temporelles et l'ampleur des débits printaniers à une échelle spatiale suffisante pour la gestion des bassins hydrographiques. Dans cette étude, le modèle

Robert P. Larson, James M. Byrne, Daniel L. Johnson, Matthew G. Letts and Stefan W. Kienzle

Department of Geography, Water and Environmental Science Program, University of Lethbridge, 4401 University Dr., Lethbridge, Alberta, T1K 3M4

Submitted January 2010; accepted October 2010. Written comments on this paper wil be accepted until September 2011.

de microclimats simulés « SIMGRID » a été raffiné et appliqué à la simulation de l'équivalent en eau de la neige (EEN) et au débit mesuré du printemps dans la partie amont du bassin de la rivière St. Mary au Nord du Montana. Des relations entre l'altitude et les précipitations hivernales ont été dégagées à partir de données de relevés nivométriques. L'algorithme de bilan massique de l'EEN a été amélioré pour inclure l'effet des conditions de pluie sur neige et pour distinguer le ruissellement provenant de la fonte des neiges du ruissellement provenant des pluies. Une analyse de régression multiple a été utilisée pour relier les prévisions d'EEN et de ruissellement provenant des pluies au débit observé au printemps (Q_s) à Babb, MT, pour la période 1961-1990. Le modèle SIMGRID raffiné a ensuite été appliqué à la période 1991-2004 pour simuler de façon adéquate le débit printanier (régression linéaire, r^2 = 0,67). Le modèle SIMGRID raffiné permet de simuler le ruissellement printanier sur des terrains complexes peu instrumentés, à une échelle pertinente pour la gestion des ressources en eau. Cet article présente les résultats de la partie I d'une étude en deux parties, qui évalue les impacts du changement climatique sur le ruissellement printanier pour le bassin d'étude.

Introduction

Spring snowmelt accounts for 70-90% of the annual flow of many rivers in mountainous western North America (Stewart *et al*., 2004). Climate change is likely to alter snow accumulation and ablation patterns, with associated changes in water supply volume and timing (Barnett *et al*., 2005). Accurate snowpack and spring rainfall modeling is required to determine the direction and magnitude of long-term changes for a given watershed. Several snowpack models have been developed for mountainous terrain. Letsinger and Olyphant (2007) modeled snow cover evolution and melt in a 45 km^2 watershed in south-western Montana. Their modeled surfaces compared well with satellite images for one year. ALPINE3D (Lehning *et al*., 2006), SnowModel (Liston and Elder, 2006), and ISNOBAL (Marks *et al*., 1999) are other examples of high resolution hydrologic models applied to diverse terrain. They incorporate detailed snowpack processes, including sublimation and snow redistribution (Bowling *et al*., 2004; Pomeroy and Li, 2000; Winstral and Marks, 2002), as well as canopy interception and associated energy balance variations (Link and Marks, 1999; Lundberg and Koivusalo, 2003; Pomeroy *et al*., 1998). These models represent important advances in our understanding of the physical processes determining snow cover distribution and streamflow generation, but they often require extensive field instrumentation for development and verification (Pagano *et al*., 2005). Such models are best suited to research applications in relatively small watersheds.

In watersheds of sufficient size for water management applications, accurate streamflow simulation has been achieved by linking high resolution hydrology models with streamflow modules that rely on statistical interpolation of meteorological data from stations near and within the watershed. For example, Garen and Marks (2005) coupled ISNOBAL with a streamflow simulation model, to simulate discharge from a 2150 km^2 watershed. Meteorological input for their model was obtained from wind, radiation and humidity sensors from a network of meteorological stations in the vicinity of the watershed. A number of spatial interpolation models have been developed for this purpose, but performance is strongly related to the density of weather station networks (Daly, 2006; Daly *et al*., 2007), especially in smaller watersheds where there may be few, if any, stations available (Diaz, 2005).

The objective of this paper was to further develop, calibrate and evaluate a distributed daily snow and rain-on-snow model for application in the St. Mary River watershed. This 554 km^2 catchment is located along the eastern slopes of the Rocky Mountains in Glacier National Park, northern Montana (MT). A snow hydrology modeling approach was used, incorporating spatial and temporal scales relevant to water management interests. Complex terrain, as observed in the St. Mary catchment, is known to play an important role in the spatial and temporal variability of snow water equivalent (SWE) spatial fields (Elder *et al*., 1998; Letsinger and Olyphant, 2007). Dense measurement networks would also be required for effective spatial interpolation of daily weather data, but there is only one climate station in the watershed. To address the issue of sparse weather data availability, the ability of a refined SIMGRID model to simulate

SWE, rainfall runoff and streamflow throughout the watershed is tested in this paper, using a model that extrapolates daily weather data throughout the catchment from a single weather station, according to basic meteorological principles.

A spatially-distributed SWE mass balance model (see Lapp *et al.*, 2005; Shepperd, 1996) based on the MTCLIM Model (Hungerford *et al.*, 1989) was adopted and refined. The daily SWE melt and rain-on-snow events were linked to historical spring runoff volumes for the period 1961-1990, using multiple linear regression techniques. Finally, the model performance was tested by simulating spring streamflow for the 1991-2004 period. The purpose of this first part of a two-part study was to develop a model that could be used to project changes in spring runoff volume through the end of the 21st Century (Larson *et al.*, this issue).

To achieve the objective of Part I of this study, the following steps were taken:

- Verify the MTCLIM Model air temperature output at 1900 metres above sea level (masl), using microclimate data from the Lakeview Ridge, Glacier-Waterton International Peace Park, near Waterton Lakes, AB, Canada.
- Formulate a watershed-specific algorithm relating elevation to precipitation, based on snow survey SWE data, and link it into the model using the St. Mary, MT, USA, climate data as the model input.
- Refine the snow accumulation algorithm to account for rain-on-snow, which is critical during the spring melt period and for the study area.
- Compile the modeled data for the 1961-1990 water years and calibrate spring runoff regressions according to observed spring streamflow volumes at Babb, MT.
- Use the model to simulate spring runoff volumes for the 1991-2004 period and compare modeled output to recorded streamflow data for the same period.

Study Area

The study area lies on the eastern slopes of the Montana-Alberta Rockies (Figure 1). The watershed comprises a large portion of the headwaters of the St. Mary River

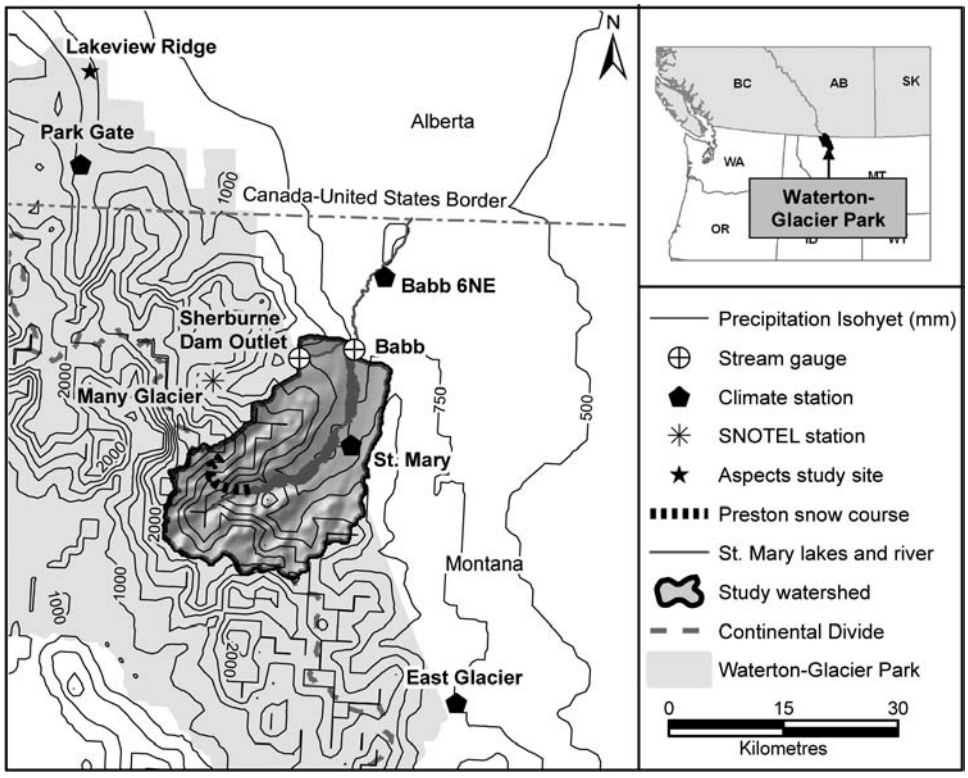

Figure 1. The study watershed lies mostly within Waterton- Glacier International Peace Park (inset).

basin, which supplies water for irrigation of more than 200,000 ha in Montana and Alberta. The St. Mary River headwaters cover much of the Waterton-Glacier International Peace Park, where local relief extends from 1200 m (all elevations are metres above sea level, unless otherwise noted) foothills to mountain peaks over 3000 m. Runoff from the study region feeds the Upper and Lower St. Mary lakes in Montana, before crossing the USA-Canada border north-eastward to eventually join the Saskatchewan River, and finally draining to Hudson Bay.

The study catchment includes the region upstream from the Babb gauging station, minus the portion upstream of the Lake Sherburne Dam outlet gauging station (Figure 1). Gauge data from the Lake Sherburne Dam was used to obtain naturalized streamflows for the watershed area above the Babb hydrometric station, but below the dam. Land surface classes are 35% coniferous forest (lodgepole pine, white spruce, Douglas-fir), 25% deciduous and herbaceous vegetation, 20% bare rock or soil, and 4% open water (Montana Natural Resource Information System (MNRIS), 2006). Basin slopes, determined with a 10 m × 10 m DEM, range from 0 to 75˚. Basin elevation, aspect and slope data are provided in Table 1.

The study area is a sharply transitional zone between northern Pacific coastal and continental climates because of the Rocky Mountain divide which runs orthogonally to the prevailing westerlies. In winter (October-March), the Pacific influence dominates, resulting in frequent cloudiness and precipitation. At higher elevations, snowfall contributes about 70% of the total annual precipitation (Selkowitz *et al*., 2002). The orographic effect is strong on the west side of the Continental Divide, and mountain locations east of the Divide are subject to precipitation "blow-over" (Finklin, 1986). Annual mean precipitation totals range between 1200 and 3000 mm in the alpine regions, but quickly taper to 450 to 500 mm on the plains (MNRIS, 2003). Winter precipitation at the montane Many Glacier weather station (1492 m) is more than twice that observed at the St. Mary station (1391 m), and almost seven times that observed at the lowland station at Babb (1390 m) located several kilometres east of the foothills (see Finklin, 1986; Larson, 2008: 64). Westerly Chinook, or Fœhn winds, are a dominant climatic factor on the eastern slopes, often inducing rapid snowmelt, particularly at lower elevations (Grace, 1987). Sublimation of snow during Chinook events is known to deplete snowpacks, but such losses are minimal above 1300 m (Lapp *et al*., 2005). Despite the persistent rain shadowing of the Rocky Mountain divide, the eastern slopes are also subject to orographically-enhanced precipitation, especially when moisture-laden low pressure systems pass to the south of the area in spring (Broccoli and Manabe, 1992; Reinelt, 1970).

Data used in this study included monthly precipitation from the St. Mary weather station, SWE data from the Many Glacier SNOTEL snow pillow site, and naturalized streamflow from the Babb streamflow gauging station (Figure 1). Naturalized streamflows were calculated by subtracting daily Sherburne Dam outlet streamflow from that recorded at Babb. The Sherburne Dam outlet streamflow gauge was removed in 2004; therefore, daily naturalized streamflow data could be determined at Babb for the 1961-2004 period. The St. Mary basin is located within a region with a late spring precipitation maximum, but orographic effects maintain relatively consistent precipitation depths throughout the remainder of the year (Figure 2). Snowpack begins to accumulate in October and builds until ablation exceeds accumulation in late March or early April. Streamflow volumes remain low during winter and increase with the beginning of snowmelt at low elevations. Spring streamflow volumes are assumed to be primarily driven by snowmelt runoff volume. However, spring rainfall also contributes substantially to spring streamflow volumes (Sueker *et al.*, 2000).

Modelling Approach

Mountain Microclimate Distribution

The SIMGRID program (Shepperd, 1996) extrapolates climate variables across the watershed to homogenous terrain categories (TCs). Terrain categories represent areas of equal terrain attribute combinations, and were derived from a digital elevation model (DEM). The United States Geological Survey (USGS) digital elevation model of the study watershed consists of 10 m × 10 m grid cells. Each grid cell in the watershed was reclassified into 100 m × 100 m block means, using the elevation, slope, and aspect classes shown in Table 1.

The program incorporates the Mountain Microclimate (MTCLIM) Model (Hungerford *et al*., 1989), which uses basic atmospheric physics and terrain

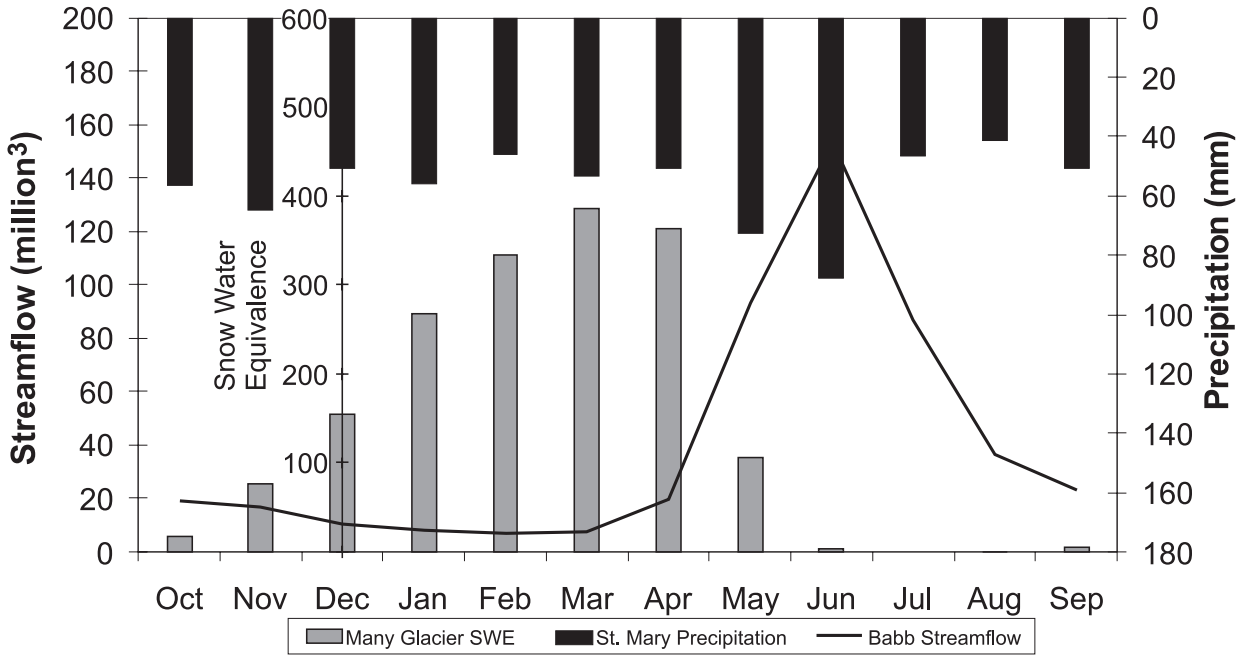

Figure 2. The study area snow hydrology is depicted through average monthly data at three stations for the overlapping period 1981-2004. Precipitation and snow water equivalent data are shown for the St. Mary and Many Glacier stations, respectively. Watershed naturalized streamflow is shown for Babb.

characteristics (e.g., elevation, aspect and slope, as above, as well as latitude and leaf area index) to estimate solar radiation, air temperature, precipitation, and relative humidity on a daily time step. The MTCLIM logic has been used in a number of studies throughout western North America (Coughlan and Running, 1997; Glassy and Running, 1994; Kimball *et al.*, 1997; Thornton *et al.*, 2000). In this study, the model extrapolates base station meteorological data from the St. Mary weather station to outlying areas (SIMGRID TCs).

The MTCLIM temperature routine was set to adjust maximum daily temperature (Tmax) using a lapse rate of -8.2 °C km^{-1} (Finklin, 1986). To account for the enhanced radiation load of sun-exposed slopes, the temperature routine adjusts Tmax according to daily solar radiation receipt on a surface of defined slope and aspect (Running *et al.*, 1987). Minimum temperature (Tmin) was adjusted by a lapse rate of -3.8 °C km^{-1}, since nighttime longwave radiation dampens the effects of complex terrain on daytime solar heating (Blennow, 1998; Thornton *et al.*, 1997). The temperature routine was validated in this study, by comparing observed and predicted values at Lakeview Ridge (1900 m). The MTCLIM model determines precipitation by comparing the ratio of annual precipitation at a given point to that at the base station. An alternative method

Table 1. Study watershed terrain classes used to group the 5,544,283 pixels into 566 Terrain Categories (TCs)

Elev. Band (m)	Area (%)	Aspect	Area (%)
1351-1450	14.43	N	2.62
1451-1550	11.58	NE	9.07
1551-1650	9.32	E	14.57
1651-1750	9.70	SE	18.31
1751-1850	9.70	S	16.53
1851-1950	8.18	SW	9.30
1951-2050	8.35	W	15.80
2051-2150	7.60	NW	13.80
2151-2250	6.43		
2251-2350	5.38	**Slope (°)**	**Area (%)**
2351-2450	4.45	0-15	49.50
2451-2550	2.72	15-30	26.19
2551-2650	1.37	30-45	18.89
2651-2750	0.54	45-60	5.07
2751-2850	0.17	60-75	0.35
2851-2950	0.06		
2951-3050	0.02		

was developed for the refined SIMGRID model, as described below. The SIMGRID outputs used in this study were daily maximum and minimum temperature, as well as precipitation values for all TCs throughout the watershed.

Snow Water Equivalent Mass Balance

Daily snow accumulation and ablation were calculated for each SIMGRID TC, using the SNOPAC program (Lapp *et al.*, 2005; Sheppard, 1996). The SNOPAC algorithms were used to partition precipitation into its liquid and solid components (Wyman, 1995) and to estimate snowmelt (Quick and Pipes, 1977). To determine snowmelt, daily temperatures were used as proxies for the three primary sources of melt energy. Convective heat transfer from warm air was represented by the mean daily temperature above freezing. Net all-wave energy flux was estimated from the daily temperature range. Lastly, latent heat gain or loss from condensation and evaporation was derived as a function of the minimum temperature, which serves as an approximation of the dew point temperature. On each day, total melt was determined as:

$$MELT = PTM \times (Tmax + TCEADJ \times Tmin) \quad (1)$$

where *PTM* is the point melt factor, which was set to 1.8 mm/day/°C (Wyman, 1995), and

$$TCEADJ = \frac{Tmin + \frac{Tr}{2}}{XTDEWP + \frac{Tr}{2}} \quad (2)$$

where *Tr* is the range between daily maximum and minimum temperatures, and *XTDEWP* is the reference dewpoint controlling energy partitioning between melt and sublimation. The *XTDEWP* parameter was set to 18°C (Wyman, 1995). Melt occurs whenever the snowpack cold storage variable *TREQ* is positive, indicating that the snowpack has ripened. *TREQ* is calculated daily, using the following temperature decay function:

$$TREQ_i = ANMLTF \times TREQ_{i-1} + Tmean_i \quad (3)$$

where $TREQ_i$ is the temperature required for melt on the ith day (°C), *ANMLTF* is a constant, set to 0.85 (see Lapp *et al.*, 2005), and $Tmean_i$ is the mean temperature on the ith day (°C).

Spring Runoff Volume

The SNOPAC program was refined to account for rain-on-snow events (SNOPAC+ROS), which are important during the spring melt season in the St. Mary basin. Total potential snowmelt runoff (S_R) and rainfall runoff (R_R) volumes were compiled from the SNOPAC+ROS program output. The variable S_R refers to the total amount of meltwater that is available for runoff or infiltration. The variable R_R refers to the amount of precipitation that occurs on saturated soils that is available for runoff or infiltration. For each year of the calibration series, S_R was determined for the period between the mean watershed date of maximum snow accumulation (*Jmax*) and the final date of snowpack disappearance (*Jdis*). R_R was determined for the period following *Jdis*. *Jmax* and *Jdis* vary across the watershed and depend on the hydrometeorology of the TCs. Watershed total SWE (*SWE*), melt (*MELT*), rainfall (*RAIN*), and watershed average Julian dates (*Jmax* and *Jdis*) were determined from TC-weighted values, as follows:

$$V_W = \frac{\sum_{i=1}^{566} V_i \times A_i}{A_W} \quad (4)$$

where, V_W is the weighted sum of a variable for the watershed, V_i is its value for the ith Terrain Category (TC), A_i is the area for the ith TC (km^2) and A_W is the study watershed area (544 km^2). For 1961-1990, the independent variables S_R and R_R were regressed against observed spring streamflow volume (Q_S). A multiple linear regression was used to model spring streamflow for 1991-2004.

The relationships between the models used in this study are shown in Figure 3. The SIMGRID model incorporates the MTCLIM model, and was used to spatially distribute the climate variables within the watershed. A precipitation-elevation relationship was formulated, and the temperature routine was verified. The SIMGRID model outputs were then input into

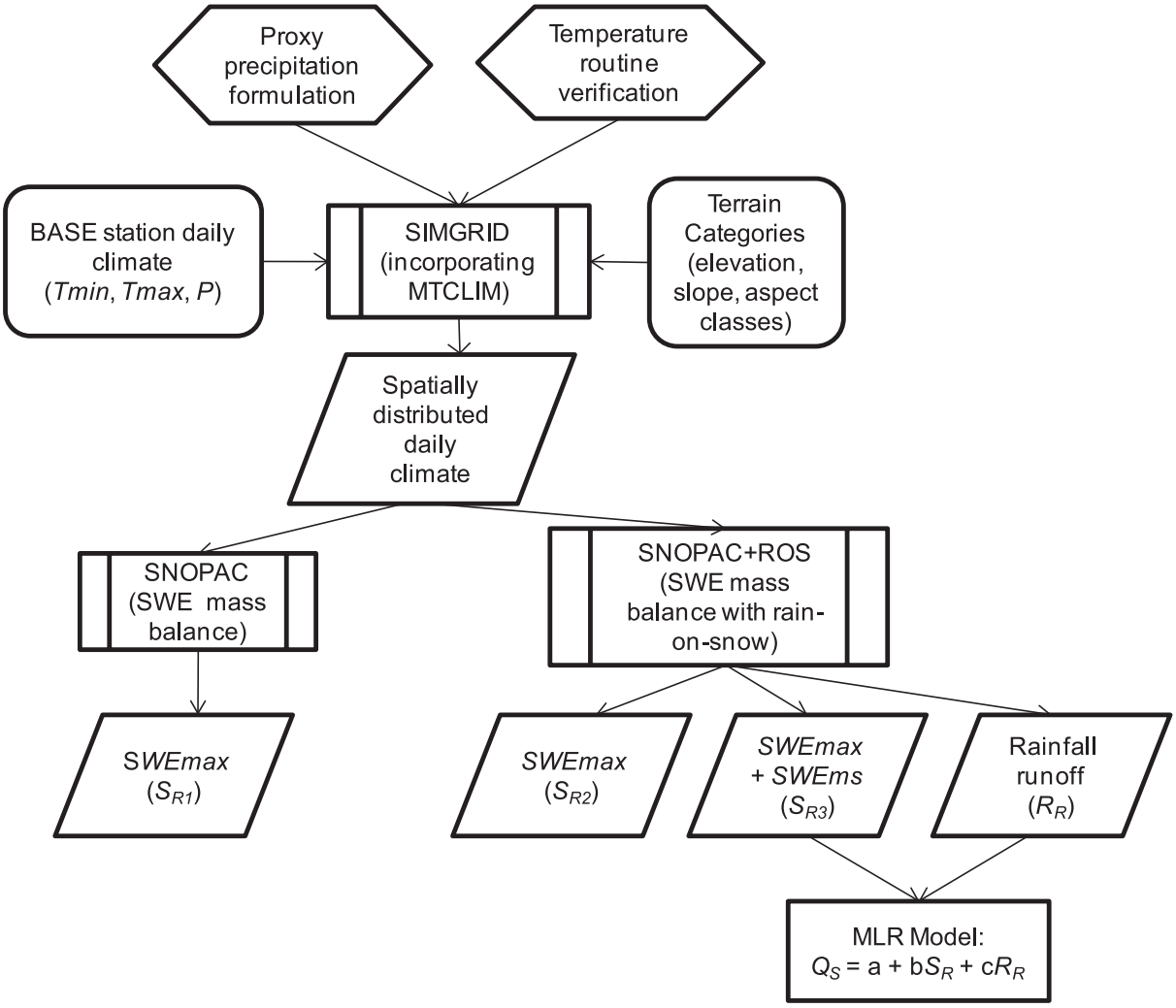

Figure 3. Modelling Approach Flow Chart

SNOPAC and SNOPAC+ROS to simulate watershed SWE and, in the case of SNOPAC+ROS, rainfall. Multiple linear regressions were conducted using output from the SNOPAC and SNOPAC+ROS programs. Observed spring streamflow was used to calibrate the model for the 1961-1990 period.

Model Refinements

Verification of the SIMGRID Temperature Routine

To evaluate the SIMGRID temperature routine, simulated maximum and minimum temperatures were compared to those observed at one metre height at three sites of contrasting aspect at elevation 1902 m, and located beneath a mountain peak along Lakeview Ridge, Glacier-Waterton International Peace Park, Alberta (Figure 1). Weather stations were located on the Northwest (NW), Southwest (SW), and Southeast (SE) aspects, as described by Letts *et al.* (2009). Data were recorded from November 26, 2005 to March 23, 2006, using HOBO (H21-001) weather loggers. The Park Gate station (1296 m elevation; Figure 1) was used as the base station for these simulations.

Analysis of observed vs. simulated values (Figure 4, Table 2) shows that there was a tendency for model underestimation of observed *Tmin* on the coldest nights and of observed *Tmax*, especially on the warmest days. Temperature underestimation on cold winter nights likely has little impact on snowmelt. The *Tmin* simulation was accurate on days with snowmelt (RMSE = 2.8°C for *Tmin* > -5 °C, without systematic bias). We, therefore, expected higher

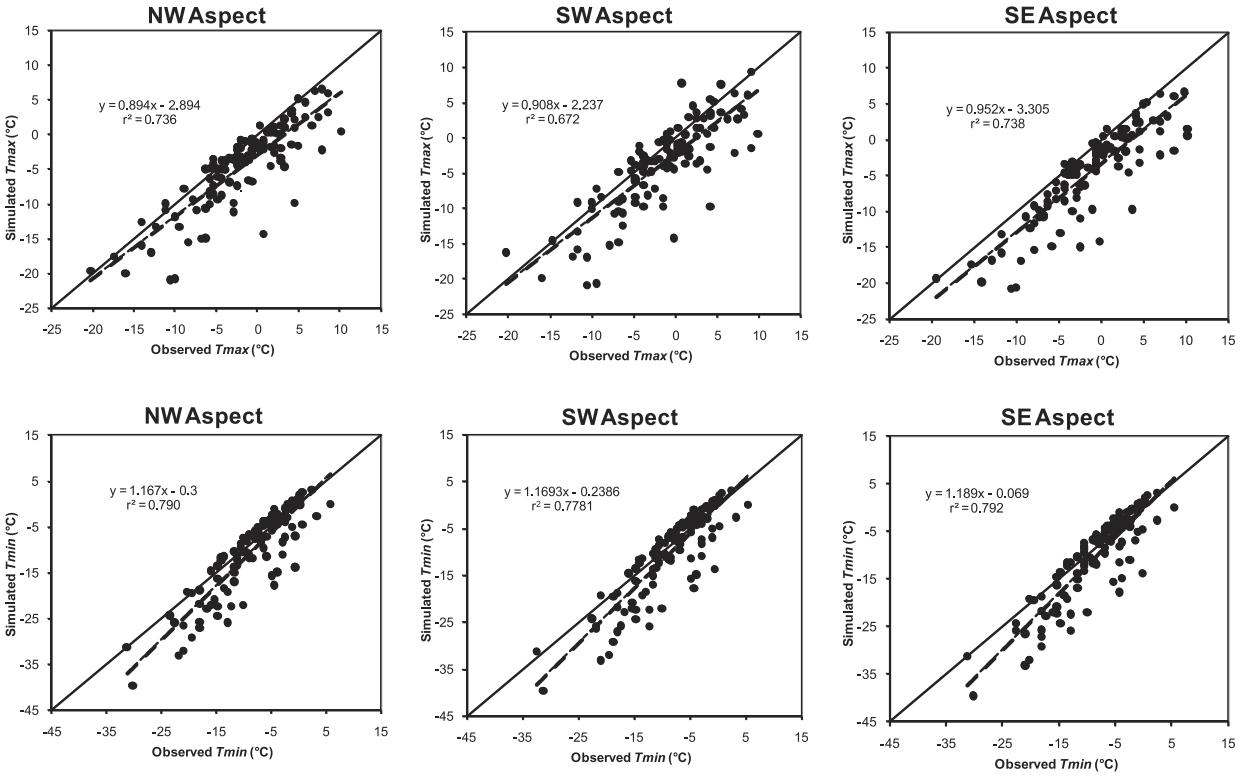

Figure 4. Daily *Tmax* and *Tmin* observed vs. simulated scatter plots for three aspects at Lakeview Ridge field site.

Table 2. Observed vs. simulated *Tmax* and *Tmin* error values at Lakeview Ridge

	Aspect	Slope (°)	RMSE (°C)	MAE (°C)
Tmax **(°C)**	SE	35	3.12	3.30
	SW	40	3.57	3.00
	NW	45	3.14	2.96
Tmin **(°C)**	SE	35	4.13	3.16
	SW	40	4.27	3.29
	NW	45	4.15	3.19

than simulated *Tmax* at Lakeview Ridge, because measurements were taken at one metre over a rocky and frequently snow-free surface. Furthermore, the use of HOBO radiation shields causes additional heating of 0.0 – 0.5°C (Nakamura and Mahrt, 2005). We elected not to adjust the SIMGRID temperature routine on the basis of results from a single site in a heterogeneous environment. However, given that underestimation of *Tmin* and *Tmax* could produce conservative estimates of climate change impacts, these results demonstrate the need for denser networks of weather stations for model verification and calibration in complex terrain.

Proxy Precipitation-Elevation Formulation

Precipitation-elevation relationships can be derived from regional climate station data (e.g. Garen and Marks, 2005), theoretical curve estimates (e.g. Thornton *et al.*, 1997), or modelled (e.g. Daly *et al.*, 1994; Hutchinson, 1995). The local precipitation-elevation relationship linked the recorded precipitation at the St. Mary climate station to observed changes in SWE. Surveyed SWE data were acquired from the Preston snow survey record for 73 dates for the period 1992 through 2006 (Fagre, 2006). The survey consists of 32 sampling locations, mainly on south and southwest aspects, at elevations from 1438 to 2290 m. Monthly snow accumulations at each specific sampling point were determined by subtracting one measurement from the previous one, as follows:

$$\Delta SWE_E^{\Delta t} = SWE_E^{t_2} - SWE_E^{t_1} \quad (5)$$

where t_2 is the snow survey date, t_1 is the date of the previous survey, and E is the sampling point local elevation (m above St. Mary climate station). Two assumptions were made in ΔSWE calculations. First, ΔSWE was assumed a proxy for cold-season precipitation for the period since the last survey. This was reasonable since most ΔSWE measurements were taken between the months of January to March, and the Preston survey points lie at a high-enough elevation to assume solid precipitation during these months. The second assumption was that melting during warm periods was equal to the difference between SWE values recorded on one survey date and those recorded on the previous date. To determine the likelihood of melt at a given sampling point, a representative lapse rate of -6.5°C km^{-1} (Barry and Chorley, 1987) was applied to the St. Mary base station air temperature record for the same time period. When the average temperature for a period was above freezing, the ΔSWE value was dropped from the dataset, based on the assumption that melt had occurred, and the surveyed change in SWE did not accurately represent precipitation over the period. In total, 31 snow survey periods were retained as positive snow accumulations for the period 1994-2006, resulting in 536 values spanning the 32 survey point elevations. The precipitation quantities recorded at the St. Mary station for each snow survey period ranged from 28 to 328 mm. Precipitation accumulations observed at the St. Mary station were matched with ΔSWE values according to time period. From these data, a relationship was developed to express the accumulated precipitation at a given elevation as a function of St. Mary station precipitation over the time period from one survey to the next, as:

$$P_E^{\Delta t} = P_{StM}^{\Delta t} + C \times E \tag{6}$$

where $P_E^{\Delta t}$ is the precipitation for a given elevation and time period (mm), $P_{StM}^{\Delta t}$ is the St. Mary precipitation for the given time period (mm), C is a constant, and E is the sampling point local elevation (m above St. Mary climate station). To obtain C, the equation was rearranged as follows:

$$\Delta P_{diff} = C \times E \tag{7}$$

where ΔP_{diff} represents the difference in precipitation at a given elevation above the St. Mary station. The orographic effect is exhibited by the ΔP_{diff} vs. elevation scatter plot (Figure 5). Specific slope and aspect

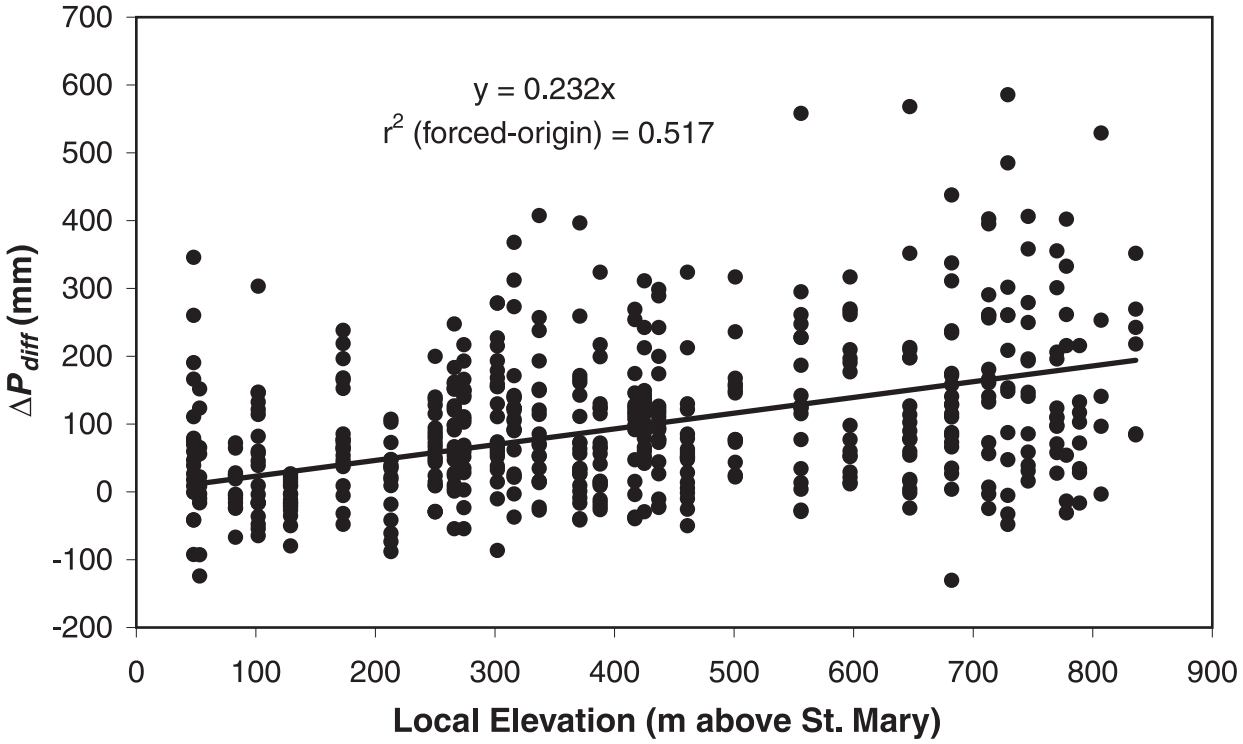

Figure 5. The variability of predicted ΔP_{diff} values, based on elevation, is shown by the scatter plot, along with the forced-origin trend line.

relationships were not detected in the data. The large degree of scatter may be due to snow redistribution.

For modelling purposes, a trend line was forced through the origin, using linear regression. To avoid creating false precipitation on dates for which no precipitation occurred at St. Mary, a constant was not included in the relationship. The distribution of standardized residuals was near-normal, indicating that the mean of the error estimates was near zero (Figure 6).

The precipitation-elevation relationship was derived based on approximately monthly snow accumulation data. To apportion the monthly accumulation to a daily time step, a ΔP_{StM} ratio was incorporated into the SIMGRID precipitation routine:

$$P_E^i = P_{StM}^i + 0.232 \times E \times \left(\frac{P_{StM}^i}{P_{StM}^y} \right) \quad (8)$$

where i is the time step (days), P_E^i is the precipitation on the ith day at a given elevation (mm), P_{StM}^i is the precipitation on the ith day at St. Mary, and P_{StM}^y is the sum of precipitation for the yth month, which includes the ith day.

Rain-on-Snow and Snowmelt Runoff

The snow accumulation and melt algorithm (SNOPAC) was enhanced to include rain-on-snow mass balance when the snowpack has not ripened. Rain-on-snow events occur in the cool interior Rocky Mountains as early as September when snow can occur at elevation, and as late as June, because deep snowpack persists into the warmer spring season (McCabe *et al.*, 2007). The frequency of rain-on-snow would likely increase in response to climate warming (Leung *et al.*, 2004; Loukas *et al.*, 2002). Rainfall on a cold snowpack is stored as SWE, whereas rainfall on a melting pack infiltrates and contributes to runoff (Marks *et al.*, 2001; Marks *et al.*, 2002). This distinction is important for the study area since the months exhibiting the highest rainfall coincide with the spring freshet in May and June (Figure 2). The algorithm used in the refined SNOPAC program to represent the fate of rain falling on snowpack was as follows:

$$\text{for } TREQ_i < 0;\ SWE_i = SWE_{i-1} + SNOW_i + RAIN_i \quad (9)$$

$$\text{for } TREQ_i \geq 0;\ SWE_i = SWE_{i-1} + SNOW_i - MELT_i$$

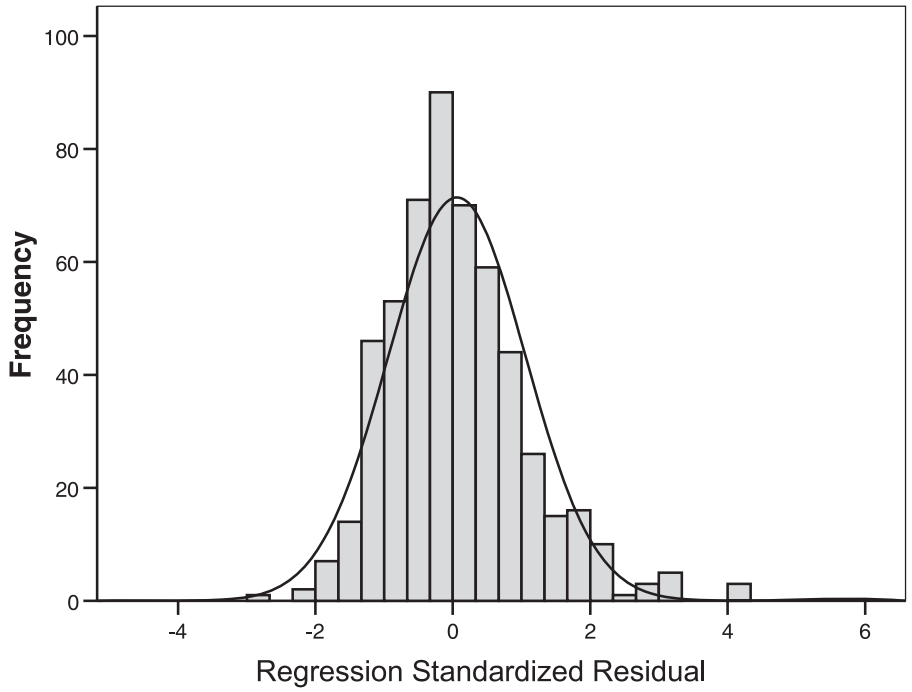

Figure 6. Standardized residuals plot of the ΔP_{diff} variable; Mean = 0.06, S = 0.998, n = 536.

where *i* is the time step (days), *TREQ* is the temperature index that must be positive for melt to occur, *SWE* is the accumulated snow water equivalent in the snowpack (mm), *SNOW* is the snowfall (mm), *RAIN* is the rainfall (mm) and *MELT* is the amount of *SWE* melted (mm). This algorithm was applied to all TCs in the watershed, and the refined program was referred to as SNOPAC+ROS. The change resulted in the discrete modeling of total potential snowmelt runoff (S_R) and total potential effective spring rainfall runoff (R_R).

To test the SNOPAC program algorithm changes, three estimates of total potential snowmelt runoff (S_R) volume were developed, as follows:

1. S_{R1} = *SWEmax* (SNOPAC); based on the maximum snow accumulation (*SWEmax*) volume determined using output from SNOPAC program;
2. S_{R2} = *SWEmax* (SNOPAC+ROS); based on the maximum snow accumulation volume determined using output from SNOPAC+ROS program;
3. S_{R3} = *SWEmax* (SNOPAC+ROS) + *SWEms* (SNOPAC+ROS); based on the maximum snow accumulation volume, and the snowfall volume occurring during the melt season (*SWEms*), determined using output from SNOPAC+ROS program.

A weighted watershed volume for each of the above was determined with Equation 4. Monthly Q_S was determined at Babb, MT, for three periods: May to July (MJJ), April to July (AMJJ), and April to August (AMJJA).

Spring Rainfall Runoff

Once the snowpack melts, soil water storage over the watershed is likely near field capacity, due to snowmelt infiltration. Therefore, for some period after the snowpack melts, a large proportion of rainfall would contribute to spring runoff. This is especially important, given that the period following snowmelt coincides with higher precipitation volumes in the project area (Figure 2). As the spring and summer progresses, however, soil water deficits develop through evapotranspiration. This results in greater infiltration and storage of rain water, and reduced runoff. To account for the enhanced rainfall runoff immediately following snowmelt, we included a potential spring rainfall runoff variable (R_R), defined for each TC as the rainfall volume occurring during a defined period (separated by 10-day increments) following the modeled Julian date of snowpack disappearance (*Jdis*). For each year, R_R volumes were summed from the modelled data corresponding to each period.

Results

To select the best of the three snowmelt runoff measures, linear regression was used to compare the three S_R variables with three observed Q_S periods (MJJ, AMJJ, and AMJJA) for the years 1961-1990. The third SWE volume measure (S_{R3}) best reflected the variability in Q_S for all spring streamflow periods (Table 3; Figure 7). There was a tendency for underestimation of *AMJJA Q*, but differences were very small in the case of $S_{R3.}$ Based on its superior performance, S_{R3} was adopted for runoff modelling during the spring snowmelt period.

The modelled date of maximum total snow accumulation (*Jmax*) was used to estimate the onset of spring streamflow at Babb. Using the watershed *Jmax* (determined by substituting with V_W in Equation 4), the spring streamflow period for each year was defined by the number of days elapsed after *Jmax*. Using the formulations for S_{R3} and R_R, the modeled Q_S time period was calculated at weekly intervals post *Jmax*, and summed to determine total spring Q_S. Model output was optimized using S_{R3} and R_R calculated for a 40-day period post *Jdis*, resulting in a 114-day period of Q_S simulation (Table 4). The final multiple linear regression equation was:

$$Q_S = -187.15 + [(0.682) \times S_R] + [(1.004) \times R_R] \quad (10)$$

The model was tested by simulating Q_S. using output from the SIMGRID and SNOPAC+ROS programs, and comparing the output with observed streamflow for 1991-2004. The spring runoff model slightly overestimated spring streamflow volume at Babb (RMSE = 50.6×10^6 m^3, R^2 = 0.668; Figure 8).

Following the positive split-sample calibration result, S_{R3} and R_{R40} were plotted against total observed Q_S for the 114-day period (Q_{S114}) over the 1961-2004 period. The coefficients for this regression were similar to those in Equation 10 (Q_S = -208.831 + [(0.701) ×

Table 3. Linear regression results evaluating the three SWE volume measures (S_R), 1961-1990 (million m³)

Variables		Equation Terms Statistics						Model Statistics	
Dependent	Independent	Constant			S_R				
Q_S period	S_R measure	a	SE_a	p_a	b	SE_b	p_b	r^2	SE_y
MJJ	1	7.913	63.288	0.901	0.666	0.126	<0.001	0.498	53.723
	2	-14.456	65.952	0.828	0.707	0.131	<0.001	0.510	53.099
	3	**-88.955**	**61.711**	**0.161**	**0.638**	**0.091**	**<0.001**	**0.635**	**45.832**
AMJJ	1	29.794	60.694	0.627	0.659	0.121	<0.001	0.514	51.520
	2	7.119	63.092	0.911	0.700	0.125	<0.001	0.528	50.796
	3	**-65.206**	**58.685**	**0.276**	**0.630**	**0.087**	**<0.001**	**0.652**	**43.585**
AMJJA	1	28.832	65.595	0.664	0.737	0.131	<0.001	0.531	55.681
	2	2.787	67.976	0.986	0.785	0.135	<0.001	0.547	54.728
	3	**-79.571**	**61.931**	**0.209**	**0.708**	**0.092**	**<0.001**	**0.680**	**46.000**

"a" is the constant (intercept) and "b" is the coefficient (slope) of the linear model.
"SE" is the standard error for each term within the linear model.
"p" is the p-value for each term within the linear model.

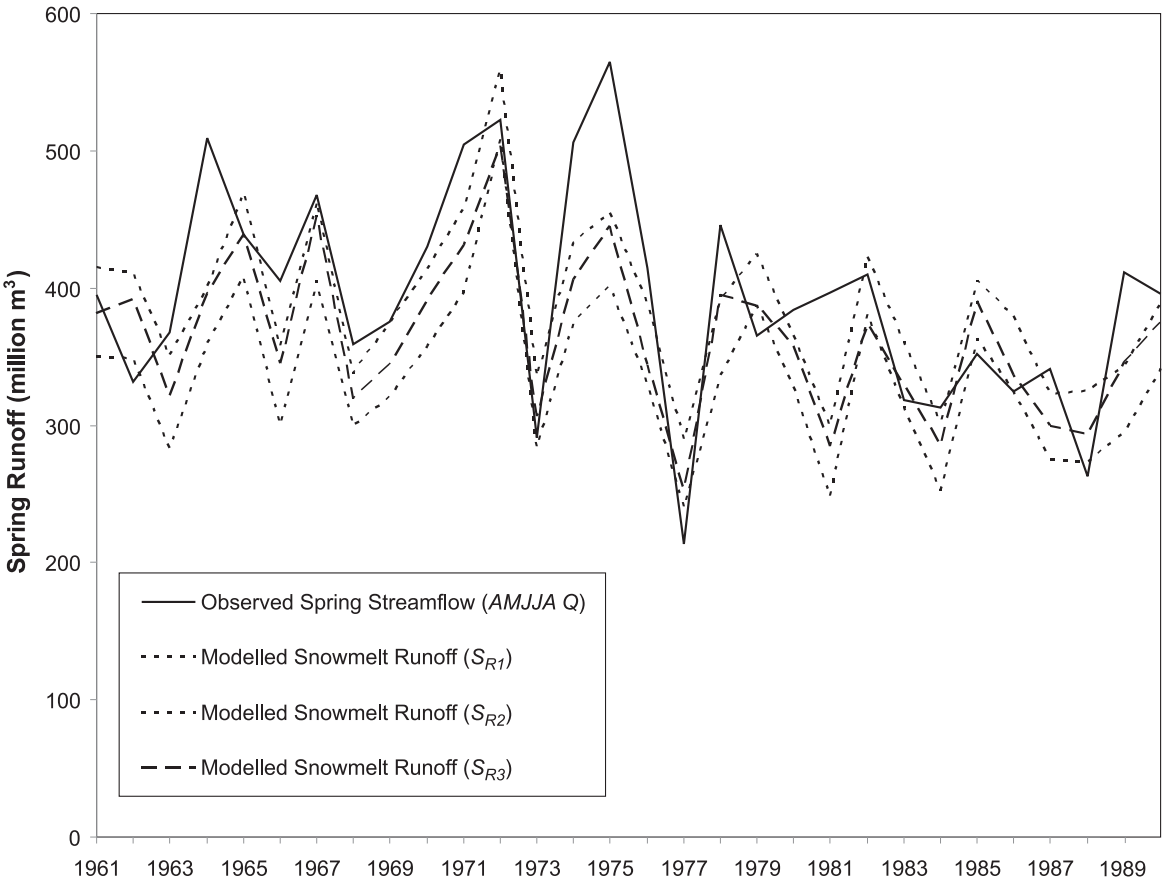

Figure 7. Observed and modelled Spring Runoff for April to August (*AMJJA Q*), 1961-1990. The three SWE volume measures (S_{R1}, S_{R2}, and S_{R3}) are shown, along with the observed spring streamflow volume (Q_S).

S_R] + [(1.072) × R_R]. The forced-origin trend line of the observed versus modelled Q_S had a slope close to one (m = 0.987, SE = 0.017), indicating no systematic deviation from the expected 1:1 relationship (t = -0.779, p = 0.440; Figure 9). However, variability in Q_S was greater for years with high Q_S. The independent, mass balance-based S_R and R_R variables were not significantly correlated (Pearson's r = 0.228, p = 0.137, n = 44).

Table 4. Best model results from multiple linear regressions using the third SWE measure (S_R), along with the R_R and Q_S variables, 1961-1990 (million m³)

Variables			Equation Terms Statistics									Model Statistics	
Independent		Dependent	Constant			SR			RR				
S_R measure	R_R period (days)	Q_S period (days)	a	SE_a	p_a	b	SE_b	p_b	c	SE_c	p_c	R2	SEy
		107	-219.34	61.45	0.002	0.740	0.090	<0.001	0.803	0.381	0.044	0.751	44.40
3	30	114	-194.35	61.30	0.004	0.742	0.090	<0.001	0.746	0.380	0.060	0.750	44.30
		121	-183.82	61.70	0.006	0.747	0.091	<0.001	0.707	0.382	0.075	0.748	44.58
		107	-203.57	54.78	0.001	0.680	0.086	<0.001	1.031	0.311	0.003	0.793	40.41
3	40	114	**-187.15**	**54.44**	**0.002**	**0.682**	**0.085**	**<0.001**	**1.004**	**0.309**	**0.003**	**0.794**	**40.16**
		121	-177.56	54.91	0.003	0.687	0.086	<0.001	0.979	0.312	0.004	0.792	40.50
3	50	107	-212.45	59.32	0.001	0.703	0.091	<0.001	0.774	0.308	0.018	0.764	43.15
		114	-194.34	61.30	0.004	0.742	0.090	<0.001	0.746	0.380	0.060	0.750	44.30
		121	-183.82	61.69	0.006	0.747	0.091	<0.001	0.707	0.382	0.075	0.748	44.58

"a" is the constant (intercept), and "b" and "c" are the coefficients of the multiple linear model

"SE" is the standard error for each term within the multiple linear model

"p" is the p-value for each term within the multiple linear mode

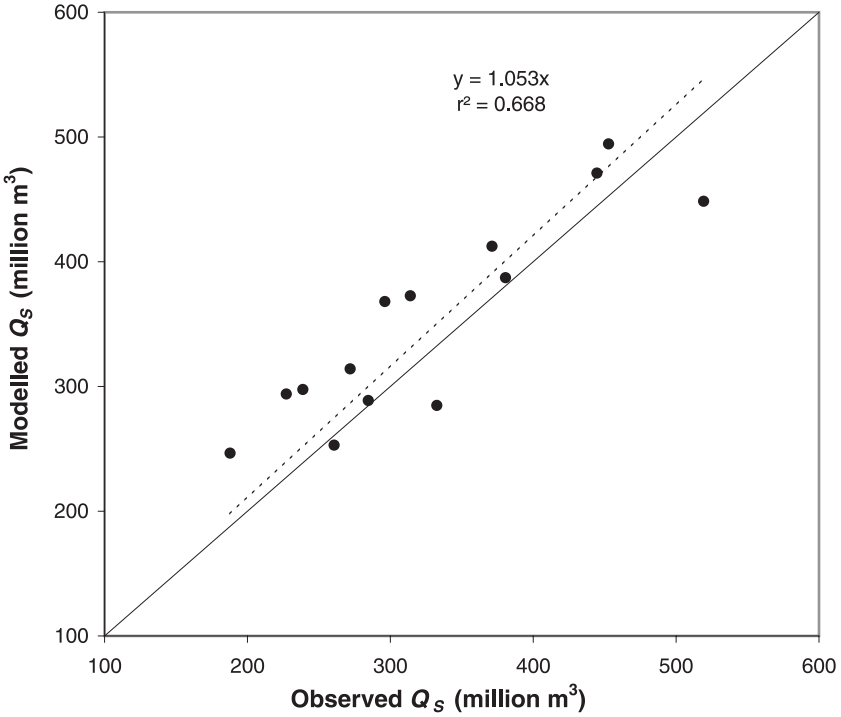

Figure 8. Observed versus modelled Q_S scatter plot for the 1991-2004 period. A 1:1 line is included.

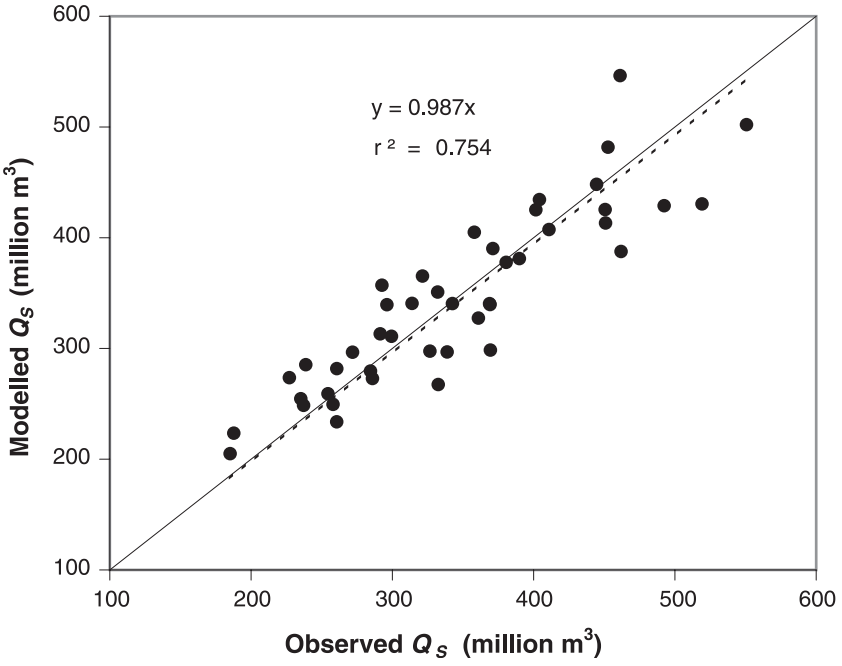

Figure 9. Observed versus modelled Q_s scatter plot, 1961-2004 water years, including the 1:1 line.

The stepwise regression analysis for the 1961-2004 data revealed that S_R accounted for 70% of the variability in Q_S, while R_R accounted for an additional 9%. As expected, snowmelt runoff was a much more important factor in determining spring streamflow, but the spring rainfall is also statistically significant in determining total spring runoff. Overall, the spring streamflow volume predicted by Q_S accounted for 72% of the cumulative streamflow volume at Babb for the period 1961-2004. This demonstrates the importance of modelling the snow hydrology system in alpine watersheds, and the relevance of this model to water supply management.

Summary and Conclusion

Results demonstrate that distributed models based on daily snow, rain-on-snow and spring rainfall can effectively simulate spring snowmelt runoff in complex terrain. These models can be run at scales applicable to watershed management, even in regions with sparse meteorological data. The strong correlation between observed and simulated 1961-2004 streamflow strongly suggests that the model may be used to provide approximations of water supply volume and runoff timing changes in response to future climate scenarios, though results should be analyzed with care as future temperature and precipitation values may fall outside of the range for which the streamflow model was developed. The model developed and presented here, named SIMGRID Snow-Runoff, is used in part II of this study to assess changes in spring runoff in response to future scenarios of climate change.

Acknowledgements

This work was funded by the Alberta Ingenuity Centre for Water Research under Theme 1 (Watersheds). We would like to thank the USGS West Glacier Field Station (West Glacier, Montana) and Dr. Dan Fagre for snow survey and DEM data. We appreciate the many comments received from anonymous reviewers, which helped to improve the manuscript. Many thanks are owed to various individuals who helped with miscellaneous tasks.

References

Barnett, T. P., J. C. Adam, and D. P. Lettenmaier. 2005. Potential impacts of a warming climate on water availability in snow-dominated regions. Nature 438(17): 1-7.

Barry, R. G., and R. J. Chorley. 1987. *Atmosphere, Weather and Climate*, 5th ed., 448 pp., Methuen and Co. Ltd., New York.

Blennow, K. 1998. Modelling minimum air temperature in partially and clear felled forests. *Agricultural and Forest Meteorology* 91(3-4): 223-235.

Bowling, L. C., J. W. Pomeroy, and D. P. Lettenmaier. 2004. Parameterization of Blowing-Snow Sublimation in a Macroscale Hydrology Model. *American Meteorological Society* 5: 745-761.

Broccoli, A. J., and S. Manabe. 1992. The Effects of Orography on Midlatitude Northern Hemisphere Dry Climates. *Journal of Climate* 5(11): 1181-1201.

Coughlan, J., and S. W. Running. 1997. Regional ecosystem simulation: A general model for simulating snow accumulation and melt in mountainous terrain. *Landscape Ecology* 12(3): 119-136.

Daly, C. 2006. Guidelines for assessing the suitability of spatial climate data sets. *International Journal of Climatology* 26: 707-721.

Daly, C., R. P. Neilson, and D. L. Phillips. 1994. A Statistical-Topographic Model for Mapping Climatological Precipitation over Mountainous Terrain. *Journal of Applied Meteorology* 33: 140-158.

Daly, C., J. W. Smith, and J. I. Smith. 2007. High-resolution spatial modeling of daily weather elements for a catchment in the Oregon Cascade Mountains, United States. *Journal of Applied Meteorology and Climatology* 46: 1565-1586.

Diaz, H. F., 2005. Monitoring climate variability and change in the western United States, in *Global Change and Mountain Regions*, edited by U. M. Huber, *et al*., pp. 267-273, Springer, Dordrecht, The Netherlands.

Elder, K., W. Rosenthal, and R. E. Davis. 1998. Estimating the spatial distribution of snow water equivalence in a montane watershed. *Hydrological Processes* 12: 1793-1808.

Fagre, D. 2006. Unpublished USGS data from the Climate Change in Mountain Ecosystems project at Glacier National Park. United States Geological Survey (USGS). West Glacier, Montana.

Finklin, A. I. 1986. *A climatic handbook of Glacier National Park —with data for Waterton Lakes National Park* 55 pp, USDA Forest Service Ogden, UT.

Garen, D. C., and D. Marks. 2005. Spatially distributed energy balance snowmelt modelling in a mountainous river basin: estimation of meteorological inputs and verification of model results. *Journal of Hydrology* 315(1-4): 126-153.

Glassy, J. M., and S. W. Running. 1994. Validating Diurnal Climatology Logic of the MT-CLIM Model Across a Climatic Gradient in Oregon. *Ecological Applications* 4(2): 248-257.

Grace, B. W., 1987. Chinooks. *Chinook* 9: 52-56.

Hungerford, R. D., R. R. Nemani, S. W. Running, and J. C. Coughlan. 1989. *MTCLIM: Mountain Microclimate Simulation Model. Research Paper INT-414*, 52 pp, U.S. Department of Agriculture, Forest Service, Intermountain Research Station, Ogden, UT.

Hutchinson, M. F. 1995. Interpolating mean rainfall using thin plate smoothing splines. *International Journal of Geographical Information Systems* 9: 385-403.

Kimball, J. S., S. W. Running, and R. Nemani. 1997. An improved method for estimating surface humidity from daily minimum temperature. *Agricultural and Forest Meteorology* 85(1-2): 87-98.

Lapp, S., J. M. Byrne, S. W. Kienzle, and I. Townshend. 2005. Climate warming impacts on snowpack accumulation in an alpine watershed: A GIS based modeling approach. *International Journal of Climatology* 25(4): 521-526.

Larson, R.P. 2008. Modelling Climate Change Impacts on Mountain Snow Hydrology, Montana-Alberta. M.Sc. Thesis, 136 pp, University of Lethbridge, Lethbridge.

Larson, R. P., J. M Byrne, D. L. Johnson, S. W. Kienzle, M. G. Letts. this issue. Modelling Climate Change Impacts on Spring Runoff for the Rocky Mountains of Montana and Alberta II: Future Scenarios and Runoff Change Forecasts. *Canadian Water Resources Journal* 36(1): 35-52.

Lehning, M., I. Völksch, D. Gustafsson, T. A. Nguyen, M. Stähli, and M. Zappa. 2006. ALPINE3D: a detailed model of mountain surface processes and its application to snow hydrology. *Hydrological Processes* 20(10): 2111-2128.

Letsinger, S. L., and G. A. Olyphant. 2007. Distributed energy-balance modeling of snow-cover evolution and melt in rugged terrain: Tobacco Root Mountains, Montana, USA. *Journal of Hydrology* 336: 48-60.

Letts, M. G., K. N. Nakonechny, K. E. V. Gaalen, and C. M. Smith. 2009. Physiological acclimation of Pinus flexilis to drought stress on contrasting slope aspects in Waterton Lakes National Park, Alberta, Canada. *Canadian Journal of Forest Research* 39(3): 629-641.

Leung, L. R., Y. Qian, X. Bian, W. M. Washington, J. Han, and J. O. Roads. 2004. Mid-century ensemble regional climate change scenarios for the western United States. *Climatic Change* 62: 75-113.

Link, T. E., and D. Marks. 1999. Point simulation of seasonal snow cover dynamics beneath boreal forest canopies. *Journal of Geophysical Research* 104(D22): 27 841–827 858.

Liston, G. E., and K. Elder. 2006. A distributed snow-evolution modeling system (SnowModel). *Journal of Hydrometeorology* 7: 1259-1276.

Loukas, A., L. Vasiliades, and N. R. Dalezios. 2002. Potential climate change impacts on flood producing mechanisms in southern British Columbia, Canada using the CGCMA1 simulation results. *Journal of Hydrology* 259(1-4): 163-188.

Lundberg, A., and H. Koivusalo. 2003. Estimating winter evaporation in boreal forests with operational snow course data. *Hydrological Processes* 17(8): 1479-1493.

Marks, D., J. Domingo, D. Susong, T. Link, and D. Garen. 1999. A spatially distributed energy-balance snowmelt model for application in mountain basins. *Hydrological Processes* 13: 2439-2452.

Marks, D., T. Link, A. Winstral, and D. Garen. 2001. Simulating snowmelt processes during rain-on-snow over a semi-arid mountain basin. *Annals of Glaciology* 32: 195-202.

Marks, D., A. Winstral, and M. Seyfried. 2002. Simulation of terrain and forest shelter effects on patterns of snow deposition, snowmelt and runoff over a semi-arid mountain catchment. *Hydrological Processes* 16(18): 36-05-3626.

McCabe, G. J., M. P. Clark, and L. E. Hay. 2007. Rain-on-snow events in the western United States. *Bulletin of the American Meteorological Society* 88: 319-328.

Montana Natural Resource Information System (MNRIS). 2003. St. Mary watershed PRISM precipitation map, Accessed June 16, 2009. http://nris.mt.gov/gis/gisdatalib/downloads/precip_10010002.pdf., Spatial Analysis Climate Service, Oregon State University.

Montana Natural Resource Information System (MNRIS). 2006. National Land Cover Data for Montana, Accessed February 15, 2006. http://nris.mt.gov/nsdi/nris/nlcdgrid.html., United States Geological Survey (USGS).

Nakamura, R. and L. Mahrt. 2005. Air temperature measurement errors in naturally ventilated radiation shields. *Journal of Atmospheric and Oceanic Technology* 22(7): 1046-1058

Pagano, T. C., J. Erxleben, and T. Perkins. 2005. Operational simulation modeling at the NRCS National Water and Climate Center, paper presented at Western Snow Conference.

Pomeroy, J. W., and L. Li. 2000. Prairie and arctic areal snow cover mass balance using a blowing snow model. *Journal of Geophysical Research* 105(D21): 26 629–626 634.

Pomeroy, J. W., J. Parviainen, N. Hedstrom, and D. M. Gray. 1998. Coupled modelling of forest snow interception and sublimation. *Hydrological Processes* 12: 2317-2337.

Quick, M. C., and A. Pipes. 1977. UBC watershed model. *Hydrological Sciences Bulletin* 22: 153-162.

Reinelt, E. R. 1970. On the role of orography in the precipitation regime of Alberta. *Albertan Geographer* 6: 45-58.

Running, S. W., R. R. Nemani, and R. D. Hungerford. 1987. Extrapolation of synoptic meteorological data in mountainous terrain and its use for simulating forest evapotranspiration and photosynthesis. *Canadian Journal of Forest Research* 17: 472-483.

Selkowitz, D. J., D. B. Fagre, and B. A. Reardon. 2002. Interannual variations in snowpack in the Crown of the Continent Ecosystem. *Hydrological Processes* 16: 3651-3665.

Shepperd, A. 1996. Modelling Hydrometeorology in the Upper Oldman River Basin. M.Sc. Thesis, 178 pp, University of Lethbridge, Lethbridge.

Stewart, I. T., D. R. Cayan, and M. D. Dettinger. 2004. Changes in Snowmelt Runoff Timing in Western North America Under a 'Business as Usual' Climate Change Scenario. *Climatic Change* 62: 217-232.

Sueker, J. K., N. R. Kendall, and R. D. Jarrett. 2000. Determination of hydrologic pathways during snowmelt for alpine/subalpine basins, Rocky Mountain National Park, Colorado. *Water Resources Research* 36(1): 63-75.

Thornton, P. E., H. Hasenauer, and M. A. White. 2000. Simultaneous estimation of daily solar radiation and humidity from observed temperature and precipitation: an application over complex terrain in Austria. *Agricultural and Forest Meteorology* 104(4): 255-271.

Thornton, P. E., S. W. Running, and M. A. White. 1997. Generating surfaces of daily meteorological variables over large regions of complex terrain. *Journal of Hydrology* 190(3-4): 214-251.

Winstral, A., and D. Marks. 2002. Simulating wind fields and snow redistribution using terrain-based parameters to model snow accumulation and melt over a semi-arid mountain catchment. *Hydrological Processes* 16: 3585-3603.

Wyman, R. R. 1995. *Modeling Snowpack Accumulation and Depletion*, 23-30 pp, Canadian Water Resources Association (CWRA), Vancouver, BC.